4th Specialty Conference on Coastal, Estuary and Offshore Engineering
4e Conférence spécialisée sur l'ingénierie côtière et en milieu maritime

Montréal, Québec
May 29 to June 1, 2013 / *29 mai au 1 juin 2013*

Experimental Study of Structures Subjected to Hydrodynamic and Debris Impact Forces

T. Q. Al-Faesly[1], I. Nistor[1], D. Palermo[1], and A. Cornett[2]
[1]Civil Engineering Dept. University of Ottawa, Canada
[2]Canadian Hydraulics Centre, National Research Council of Canada

Abstract: An accurate estimation of tsunami-induced forces on nearshore structures is an important step towards the design of tsunami-resilient buildings. The University of Ottawa, in collaboration with the Canadian Hydraulics Centre (CHC) of the National Research Council, located in Ottawa, has established a comprehensive experimental and numerical modeling program focusing on tsunami-structure interaction with the ultimate goal of improving tsunami mitigation methods and strategies. As part of this experimental program, the authors conducted laboratory tests on the impact of extreme hydrodynamic forces and floating debris on two structural models with different cross sections (square and circular). These structures were subjected to supercritical hydraulic bores that are similar to ones generated by broken tsunami waves advancing inland. The structural models were instrumented with sensors capable of recording time histories of the hydraulic bore depth, as well as the lateral displacement, acceleration, pressures, forces, and moments imposed on the two structural models. The bore depth and bore velocity were recorded and analyzed, and the bore-structure interaction was also investigated. The time histories of the impact force resulting from wooden debris hitting the structural models were also recorded and analyzed. The authors further investigated existing formulas provided by the most recent tsunami-resistant engineering design guideline (FEMA P-646, 2012) and the Coastal Construction Manual (FEMA P-55, 2011) to compare the experimentally-recorded hydrodynamic and debris impact forces with current prescriptions.

1 INTRODUCTION

Tsunamis have been perceived to be low-probability, highly-consequential events. Five ensuing major tsunami events (Indian Ocean 2004, Samoa Islands 2009, Solomon Islands 2010, Chile 2010, and Japan 2011) during the last decade has claimed more than 250,000 lives and caused billions of dollars in damages—raising awareness of tsunami hazards. Tsunamis generated at subduction zones are preceded by seismic ground shaking with a short lead-time: from a few minutes for a near-field source to several hours for a far-field source. Although efforts have focused on the development of efficient warning systems, inundation maps, and tsunami preparedness, the potential damage to buildings and critical coastal infrastructure lagging behind. Lessons from past tsunamis highlight the risk to critical coastal infrastructure and associated collateral damage (Indian Ocean 2004 and Japan 2011). Furthermore, these events demonstrated that in low-lying coastal regions, evacuating residents to safe higher grounds is not an option. In these situations, one possible solution is to use the upper floor levels of tsunami-resistant buildings as a vertical evacuation to minimize human casualties. Post-tsunami reconnaissance investigations to affected areas (Borrero 2005, Fujima et al. 2006, Saatcioglu et al. 2006, Chock et al. 2011, and Palermo et al. 2012) revealed that a number of buildings survived the seismic ground shaking but were damaged by the tsunami loads. They found that the hydrodynamic force and/or impact force by floating debris were the primary cause(s) of structural failure. Thus, a better understanding of tsunami-induced loads will lead to an improved design-methodology for tsunami-resistant structures. The research presented herein has investigated tsunami-bore induced forces on near-shore structural models to validate existing formulation in current design guidelines.

Lukkunaprasit et al. (2009) carried out experimental tests on a structural model at a scale of 1:100. They simulated a tsunami wave by rapidly releasing water from a head water tank. The experimental data was compared to formulas for bore velocity and hydrodynamic force available in engineering guidelines. Lukkunaprasit et al. (2009) indicated that the variable (*h)* in the velocity formula provided in both the City and County of Honolulu Building Code (CCH 2000) and Coastal Construction Manual, FEMA P-55 (2005) ($u = 2\sqrt{gh}$) should be the thickness of the leading surge tongue. This is consistent with the results of Nouri et al. (2010) that using the bore-inundation depth in the velocity formula results in an overestimation of the bore velocity. Lukkunaprasit et al. (2009) stated that "the understanding of flow behavior and characteristics based on classic dam-break problem may mislead the predictions of tsunami runup actions near the shoreline". For the quasi-steady tsunami flow, they found that using the formula suggested by FEMA P-55 ($F_d = \frac{1}{2}\rho C_d B h u^2$) offered a realistic estimation for the drag force with a drag coefficient of $C_d = 2$. Fujima et al. (2009) conducted experiments to estimate tsunami force acting on rectangular onshore structures. Two structural models were used in their study: one with a cubic shape of 100 mm side length and the other with the same dimensions except for the width along the shoreline which was doubled (200 mm). Based on their data analysis, it was concluded that for the hydrostatic force using the formula ($F_s = \alpha \rho g B h_{im}^2$) with ($\alpha = 3.3$) is more appropriate than ($\alpha = 4.5$) which was proposed by Asakura et al. (2000).

Oshnack et al. (2009) conducted large-scale experiments on simulated tsunami bores impacting a stiff wall fronted by a small seawall. The structural model was an aluminum wall 2.14 m in height and 3.66 m in width (full width of the testing flume). In this case the structural model reflected the bore; however, this was not the case in the real-field where the water flows around the structure or the structural element. Although the study found that the highest walls in the testing group were the most effective in reducing the wave force, the experimental data included some discrepancy. Arikawa (2009) implemented large-scale laboratory experiments in a long-flume (184 m) to investigate the structural performance of wood and concrete walls under the influence of hydraulic bores generated by broken solitary waves. The research illustrated that based on the strength of the wall; failure could shift from local flexural or punching shear to complete destruction of the structure. Yeom et al. (2009) analyzed the impact of a shipping container that was transported by tsunami runup with a structural element of a near-shore building. Experimental tests were conducted to calibrate a numerical model in the software program LS-DYNA. A comparison between water depth, wave force, and container drift behavior between the numerical modeling and the experimental data demonstrated the applicability of the numerical simulation to model full-scale debris impact.

2 DESIGN GUIDELINES

To date, only a handful of the design guidelines are available that specifically address tsunami forces. These include: the 2nd edition of Guidelines for Design of Structures for Vertical Evacuation from Tsunami (FEMA P-646, 2012), Japan Cabinet Office guideline (2005) (SMBTR), and City and County of Honolulu Building Code (CCH 2000). Also, the 4th edition of the Coastal Construction Manual (FEMA P-55, 2011) provides some statements for tsunami loading.

For brevity only the hydrodynamic and debris impact forces from FEMA P-55 (2011) and P-646 (2012), which represent the most recent published guidelines related to tsunami loads, will be presented.

a) Hydrodynamic force

FEAM P-55 (2011) suggests the following formula to estimate the hydrodynamic force:

[1] $F_{dyn} = \frac{1}{2} C_d \rho V^2 A$

Where F_{dyn} is the drag force acting at mid depth of inundation depth, C_d is the drag coefficient, ρ is mass density of fluid, V is the flow velocity, and A is the surface area of the structure normal to flow. FEAM P-55 recommends values for $C_d = 1.2 \text{ and } 2.0$, for circular and square piles respectively. In addition, a table for

C_d values is provided based on the width of the structure to the water depth ratio. The flow velocity is calculated considering the following two limits:

[2] $$\begin{cases} V = {}^{d_s}/_{t} & Lower\ bound \\ V = \sqrt{g d_s} & Upper\ bound \end{cases}$$

Where d_s is the still-water depth, $t = 1$ sec, and g is gravitational acceleration. The magnitude of the velocity is related to the flood zone, the coastal topography, the distance from the flooding source, and the proximity to other obstructions.

FEMA P-646 (2012) provides the following formulas to calculate the hydrodynamic force generated by a tsunami.

[3] $$F_d = \frac{1}{2}\rho_s C_d B (hu^2)_{max}$$

Where ρ_s is the fluid density including sediment , B is the width of the structure normal to flow direction, h is the flow depth, and u is the flow velocity at structure location. The term $(hu^2)_{max}$ represents the maximum momentum flux of the flow, which should be determined from detailed numerical simulation or from available inundation maps. An approximate estimate of momentum flux according to FEMA P-646 can be established from the following formula:

[4] $$(hu^2)_{max} = gR^2 \left\{0.125 - 0.235\frac{z}{R} + 0.11\left(\frac{z}{R}\right)^2\right\}$$

Where; R is the design tsunami inundation depth and z is the ground elevation at the base of the structure.
FEMA P-646 includes an impulsive force, which arises from the impact of the leading edge of a tsunami bore with a structure and it calculated as follows:

[5] $$F_s = 1.5F_d$$

F_s is the total impulsive force per unit width of the wall. Note that the impulsive load tends to be of importance to structural elements of significant width relative to the depth of the impacting bore.

b) Debris impact forces

The evaluation of the impact force that is imposed on structures by an object carried by moving water is very challenging. The Coastal Construction Manual FEMA P-55 (2011) presents the following equation to determine an impact force:

[6] $$F_i = WVC_D C_B C_{Str}$$

Where F_i is the impact force acting at the stillwater level; W is the weight of the debris; V is the flow velocity, which is approximately equals to $0.5(gd_s)^{0.5}$; and $C_D, C_B,$ and C_{Str} are the depth, blockage, and building structure coefficients, respectively. The value of the depth and blockage coefficients range from 0 to 1.0, based on the flow depth for the former and the screening level and flow path width for the latter. The third coefficient C_{Str} depends on building importance, orientation, natural period, and the impact duration. Equation (6) is a simplified form of the original provided in the commentary of ASCE 7-10.

FEMA P-646 (2012) introduced a debris impact force formula different from the previous edition as follows:

[7] $$F_i = 1.3u_{max}\sqrt{km_d(1+c)}$$

This new hybrid formula is based on the study of Haehnel and Daly (2002) and is also suggested by ASCE 7-10. The 1.3 is an importance factor that is applicable for Risk Category IV structures as identified

in ASCE 7-10. u_{max} is the maximum flow velocity at the structure location. The velocity of floating debris is assumed equal to the flow velocity and is reduced by 50% for rolling or dragging debris. k is the combined stiffness of the debris and the impacted structured, m_d is the mass of the debris, and c is the hydrodynamic mass coefficient and varies from 0 to 1 depending on the debris size and orientation. FEMA P-646 proposes $c = 1.0$ for any type of debris that is oriented transversely to the flow, while in cases of longitudinally oriented debris c has different values depending on the debris: $c = 0$ for wooden log, $c = 0.3$ for 20-ft shipping container, and $c = 0.2$ for 40-ft shipping container.

The formulas of the two guidelines were used to estimate the hydrodynamic and debris impact forces for the testing conditions of this study and compared to the experimentally recorded forces.

3 EXPERIMENTAL PROGRAM

3.1 Testing Flume

To investigate tsunami-induced bore and waterborne debris impact forces on near-shore-structures, scaled laboratory experiments were performed in a High Discharge Flume (HDF) at the Canadian Hydraulics Centre in Ottawa. The flume, made of stainless steel, has dimensions of 14.56 m in length, 2.70 m in width and 1.40 m in depth. It was equipped with a rapidly-opening swinging gate. The gate was installed such that it ensured the impoundment of a maximum volume of water of 25.50 m^3. The discharge into the flume can continuously be adjusted to 1.7 m^3/s by a variable pitch pump, where the water level is controlled by an adjustable sluice gate at the downstream end of the flume. The flume has two glass windows on one side wall to enable a visualization of the flow and video recording of the bore flow and its impact on the structural models.

3.2 Structural Models

A circular model was sized from a 9 mm thick acrylic hollow cylinder, and another square model was constructed from an acrylic sheet of 6.3 mm thickness. The models were 1.0 m in height and had a 305 mm outside cross-sectional dimension. Aluminum frames were fabricated to support the models near the base, which, in turn, were fastened to a six-degree of freedom (6DOF) high frequency load cell. The load cell was bolted to the flume bed. The 6DOF load cell permitted recording of the base shear force- and overturning moment-time histories in the flow direction and transverse to the flow. Ten pressure transducers were installed on a vertical line at the middle of the upstream face of both models to measure the pressure-time histories, Figure 1. The flow depth-time history during the tests was captured along the flume by seventeen capacitance wave gauges. Eight of the gauges were free-standing and were positioned along the flume, while the remaining was installed directly on the surface of the square and circular structural model. A high speed video camera (up to 10,000 fps) in addition to two digital video cameras were used to record the hydraulic bore behaviour, bore velocity, bore-structural model interaction, and debris flow velocity, orientation and impact with the structures.

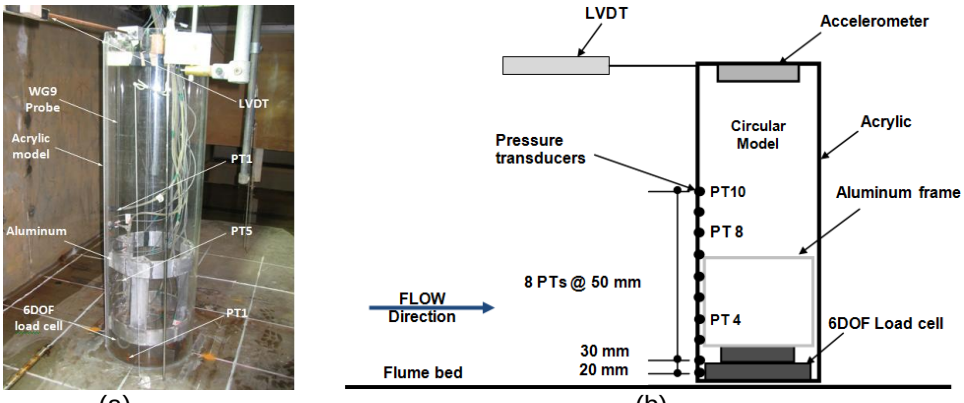

Figure 1: Circular structural model: a) installed position; and b) instrumentation details

3.3 Wooden Debris

Wooden posts of 76 mm x 76 mm in cross-sectional dimension were used to prepare three separate pieces of debris. The lengths of the debris were selected to match target masses of one and two kilograms. The corresponding lengths were 490 and 916 mm, respectively. Two pieces of 490 mm lengths were bonded together to achieve a mass of 2 kg debris. The resulting dimensions were 76 x 152 x 490 mm. All debris were coated with waterproof material to prevent saturation and changes in from the mass. The debris were designated 1kg, 2kg1P, and 2kg2P with exact masses of 1.088 kg, 2.191 kg, and 2.258 kg, respectively. Figure 2 provides the dimensions of the debris. The debris were marked with transverse lines in 100 mm intervals to enable tracking them in the high-speed video recordings. The debris speed was estimated from the time required for two successive lines on the debris to pass through a specific flume-section. For the inclined-orientation moving debris, the projection parallel to the flow direction (flume centerline) was calculated and used for velocity estimation.

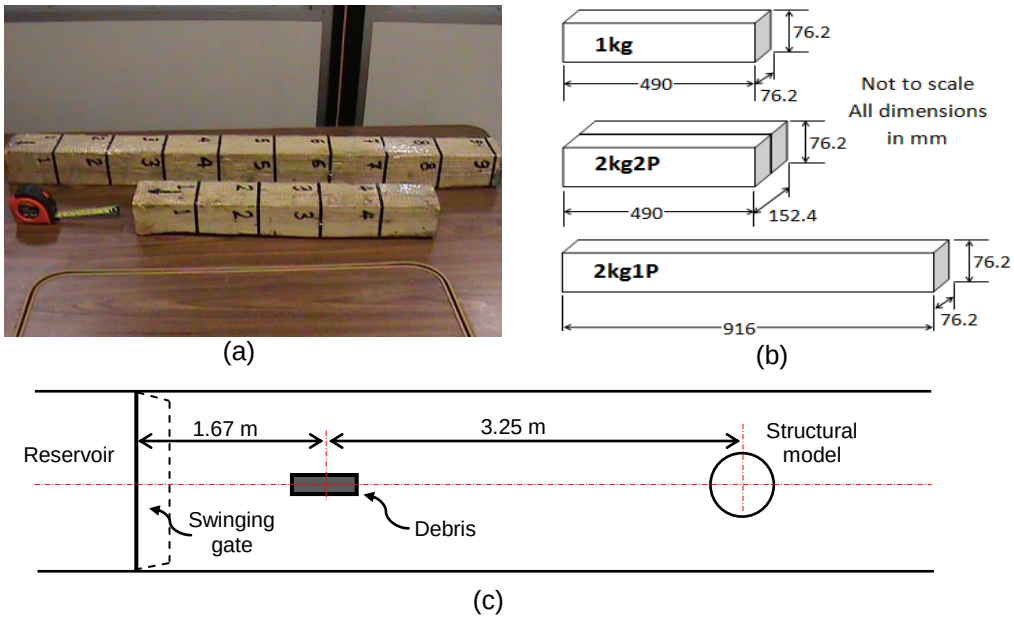

Figure 2: Wooden debris: a) dimensions; b) designations; and c) testing layout

3.4 Testing Procedure

Three impounding water depths (550, 850 and 1150 mm) were used to generate simulated tsunami bores to investigate the forces induced on the structural models. The impounding depth was monitored and controlled through a wave gauge installed in the reservoir (1.25 m upstream from the swinging gate).For the debris impact tests, two impounding water depths were used: 550 and 850 mm. To prevent damaging the structural model, the third impounding depth of 1150 mm was not investigated. The circular model only was used for these tests. Initially the debris was positioned directly on the flume bed 3.5 m upstream from the model with its longitudinal axis parallel to the flow direction. The debris was linked with two ropes that were fastened to a cross bar on the flume to avert debris from being transported into the flume reservoir. The length of the ropes was sufficient to allow the debris to impact the model freely.

Two sets of tests were conducted in the absence of the structural model in the flume with the aim of recording the bore- and velocity-time histories at the location of the model (4.92 m downstream from the swinging gate). Each test was repeated three times for each impounding water depth to ensure repeatability of the recorded test data. For the bore depth time-history test, the eight free-standing wave gauges were positioned along the flume, while for the bore velocity test, the four gauges located between the swinging gate and the model location were removed. This was implemented for two reasons: avoid suspension of seeding papers on the probes, and to reduce the discrepancy that may be caused by the gauges. The bore velocity was estimated using a particle image velocimetry (PIV) technique. The bore

was seeded with square pieces of paper approximately 30 mm in length. Two transverse bars extending across the width of the flume were used as reference markers, and were installed 150 mm upstream and downstream from the model location at a height of 480 mm from the flume bed. A wave gauge was installed at the model location to record the bore depth. The high speed camera was installed at the model location at a height of 2.4 m from the flume-bed. Given that the seed papers were near the surface of the flow, a correction of the distance travelled by the paper relative to the side makers was possible. Figures 3-a) and b) provide a drawing and photo of the test setup, respectively, while Figure 3-c) and d) provides two still frames from the high-speed video recording of a bore-velocity test with one of the seed papers crossing the reference bars. The bore was generated from a 550 mm impounding depth.

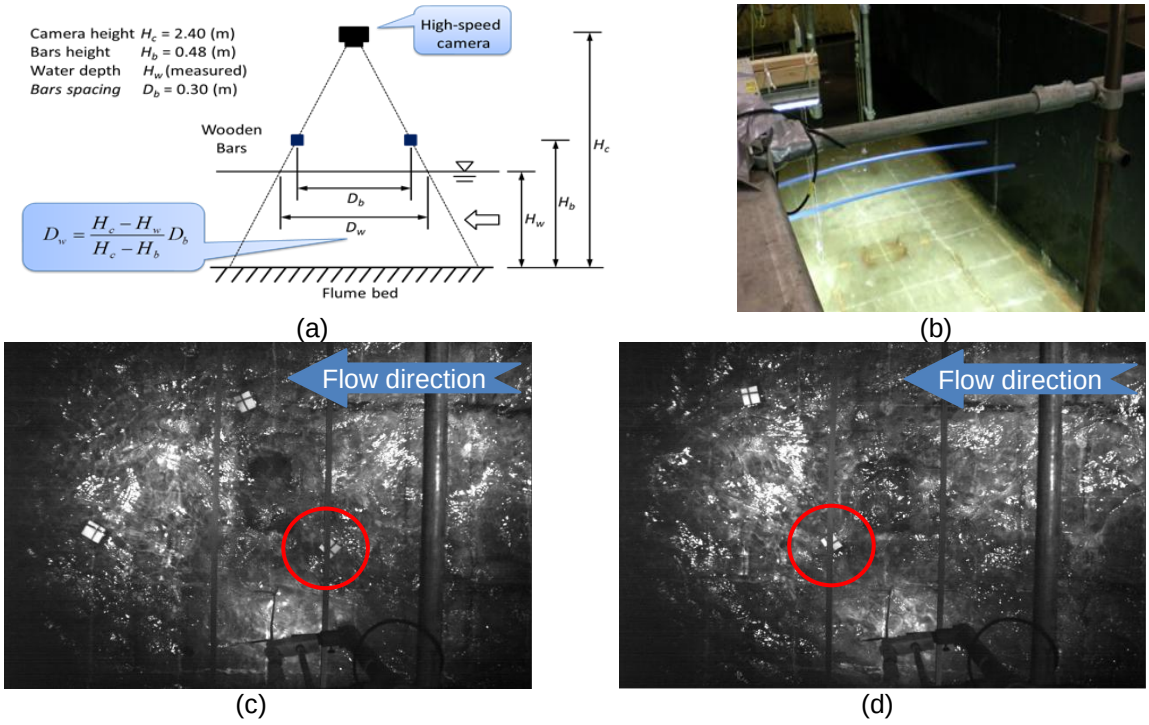

Figure 3: Bore-velocity test: a) distance correlation; b) reference bars; c) seed paper crossing 1st reference bar; and d) seed paper crossing 2nd reference bar

4 DISCUSSION OF RESULTS

4.1 Bore Depth- and Bore Velocity-Time Histories

Figure 4 shows the bore depth and bore velocity-time histories for the three impounding water depths of 550, 850 and 1150 mm. The bore depth recorded by a wave gauge (WG4) which was installed at the model location (midway between the reference bars as shown in Figure 3-b). In Figure 4, t = 0 s represents the instant the swinging gate opened and the hydraulic bore was generated. The bore front reached the model location after 1.520, 1.191 and 0.970 s for impounding water depths of 550, 850 1150 mm, respectively. The bore depth- and bore velocity-time-histories for the three impounding water depths demonstrated a similar trend. The quasi-steady flow appeared during the period from 10 s to 20 s for both the 550 mm and 850 mm impounding depths, while for 1150 mm impoundment it was recorded between 7 s to 11 s. The bore front velocities (which were the highest recorded velocities in each test) at the model location were 3.03, 4.2 and 5.02 m/s, while the quasi-steady flow velocities were 1.54, 2.19 and 2.39 m/s for the impounding water depths 550, 850 and 1150 mm, respectively. The maximum bore flow depths at the model location were 211, 292 and 344 mm for the impounding water depths 550, 850 and 1150 mm, respectively. These bore velocities and bore depths were used with the design guidelines previously presented to estimate the force components. Note that although the velocities were determined relative to the flow surface, it is assumed that they are applicable for the entire flow depth given the relatively small

flow depths investigated and the low friction of the stainless steel flume bed. Figure 4-a, b and c) reveals that as the impounding water depth increased, the slope at the leading edge of the leading to the maximum bore depth increased. In other words, the rise-time for the maximum inundation depth decreased as the impounding water depth increased. The figure concludes that as the impounding water depth increased, the bore velocity increased. For a specific impounding water depth, the velocity is a maximum at the leading edge of the bore front, and as the bore depth rises and then reaches a quasi-steady state flow level, the velocity also gradually decreases. The rate of change in the velocity decreases as the bore depth attains the steady flow level.

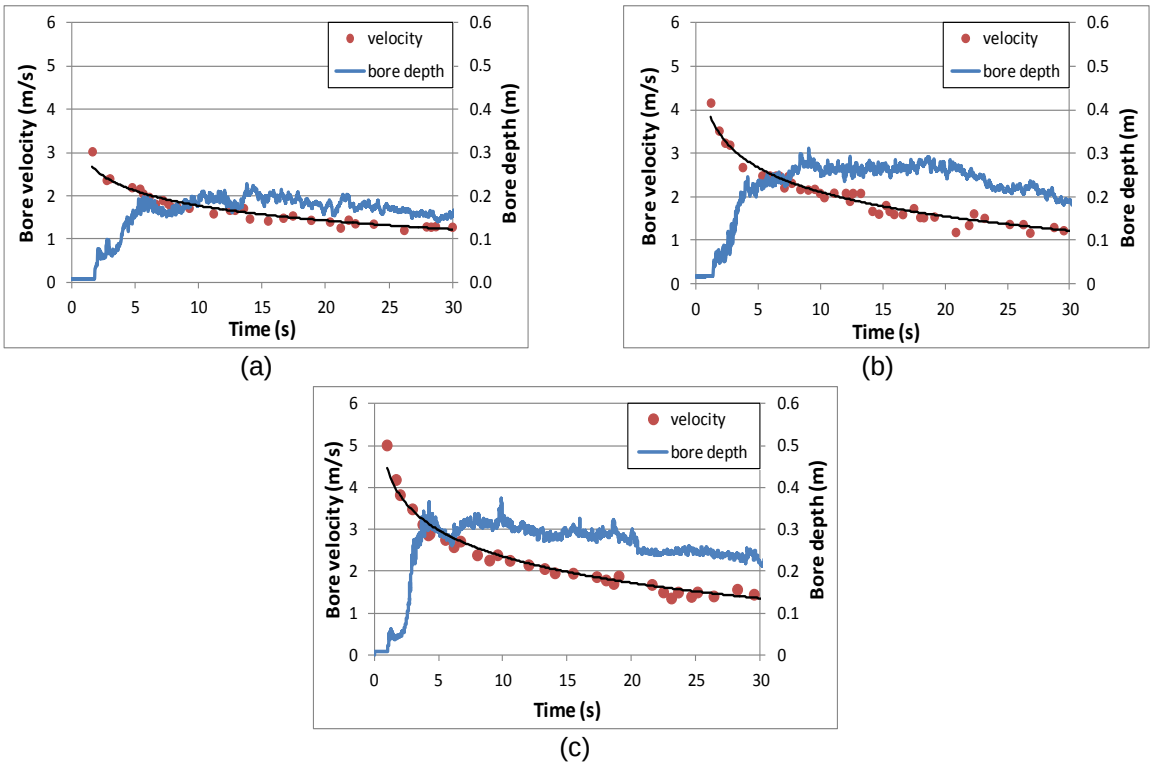

Figure 4: Bore depth and bore velocity-time histories generated by impounding depths of: a) 550 mm; b) 850 mm; and c) 1150 mm

4.2 Bore-Induced Forces

The bore-induced forces and overturning moments experienced by the structural models were recorded in the flow direction and transverse to the flow. Typical force time-histories as shown in Figure 5 and illustrates that the response is characterized by three successive stages. First stage is the impulsive force which results from the impact of the leading edge of the bore with the upstream face of the structural model. This stage consists of a very steep slope of short duration. Following the initial impulse force, there is a slight decrease in the force. The force then increases as the water builds up on the upstream face of the structural model. The force continues to increase during this second stage leading to a maximum force level known as the run-up force (transient hydrodynamic force). The flow is then redirected around the sides of the structural model until the quasi-steady flow level is attained in the third stage. Note that the run-up force is more noticeable in the square structural model, which is a direct result of the shape.

Table 1 provides the experimentally measured bore parameters and induced hydrodynamic forces on the both models with the forces estimated using the formulas provided in the design guidelines. The estimated forces using FEMA P-55 are closer to the experimental forces than the FEMA P-646, the latter significantly underestimated the forces (only 25% or less than the experimental forces). However, when

the momentum flux term $(hu^2)_{max}$ was calculated from the experimental measured bore depth and bore velocity, the output values of Eqn. 3 better match the recorded forces. For the square model, 142 N, 260 N, and 555 N; while for the circular model, 85 N, 156 N, and 333 N for impounding water depths of 550, 850 and 1150 mm, respectively, were calculated. Although these estimates are an improvement to those estimated by FEMA P-55, they still underestimate the experimental results. Using the experimentally measured parameters u and h in the hydrodynamic force formula of FEMA P-55 (Eqn.1) resulted in similar results to Eqn.3.

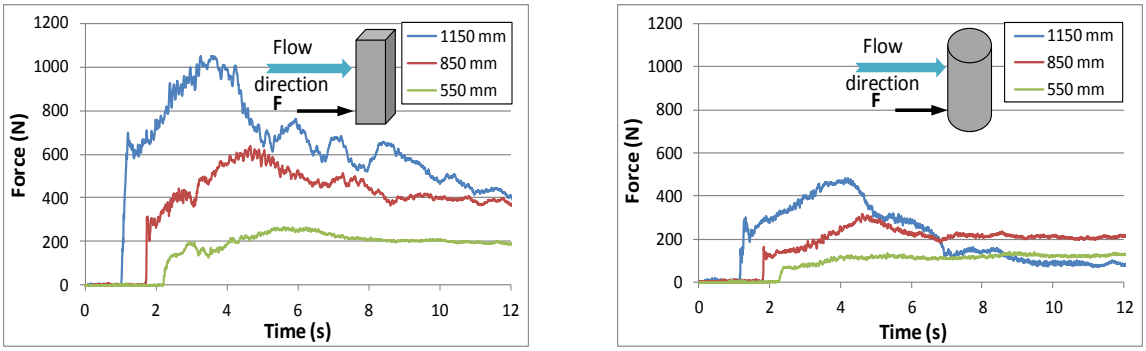

Figure 5: Bore-induced force-time histories for three impounding water levels: a) square structural model; and b) circular structural model

Table 1: Experimental and Estimated Bore-Induced Forces

Impound. depth (mm)	Water depth quasi-steady	Experimentally measured				FEMA P-55			FEMA P-646		
		u (m/s)	Max of (hu^2)	F_d (N) SQ*	F_d (N) CR*	u (m/s)	F_d (N) SQ*	F_d (N) CR*	Max of (hu^2)	F_d (N) SQ*	F_d (N) CR*
550	200	1.54	0.47	200	105	1.40	118.5	71.1	0.08	23.1	13.9
850	280	1.75	0.86	400	210	1.66	232.2	139.3	0.15	45.3	27.2
1150	330	2.36	1.84	600	305	1.80	322.5	193.5	0.25	75.0	45.0

*SQ and CR refers to the square and circular models respectively.

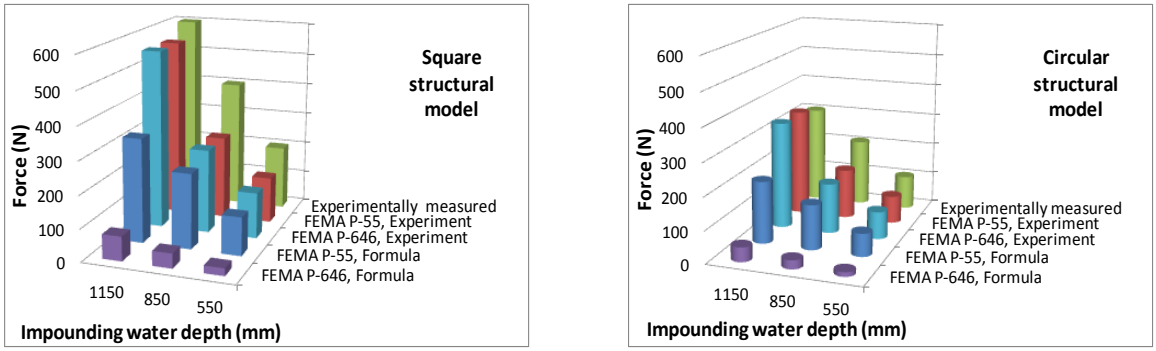

Figure 6: Comparison of hydrodynamic forces induced on structural models: a) square structural model; and b) circular model

4.3 Debris-Impact Force

Debris impact forces from three pieces of wood were investigated with two impounding water depths: 550 mm and 850 mm. The results presented are from direct impact only (longitudinal orientation). This orientation results in the largest impact force and provides a good measure against current design

guidelines. Using FEMA P-55 (Eqn.6) with the assumptions of zone V with no upstream screening, the coefficients C_D and C_B were assigned a value of 1.0. For C_{Str} three values, as described in the document, were investigated to determine which provides the most accurate impact force for this study.

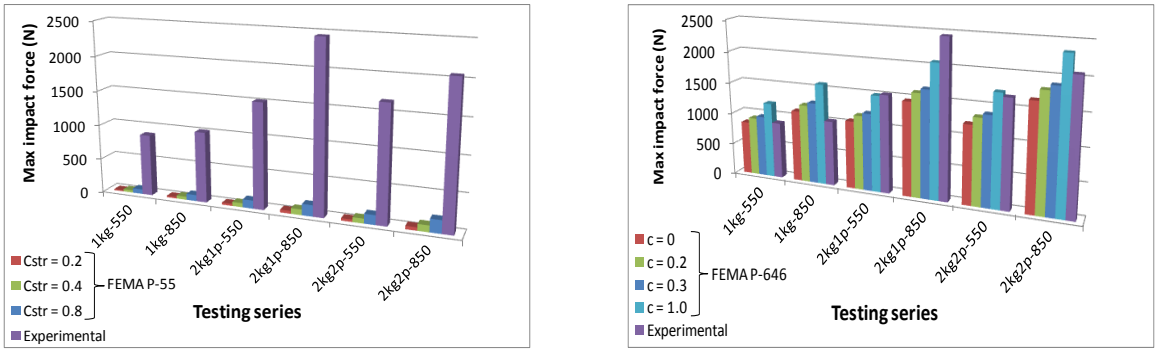

(a) (b)

Figure 7: Comparison of waterborne debris-impact force:
(a) FEMA P-55 (2011); and (b) FEMA P-646 (2012)

Figure 7-a) reveals that FEMA P-55 (2011) highly underestimates the debris impact force. Using the largest value for $C_{Str} = 0.8$ (which is intended for reinforced concrete foundation walls), the impact forces for all test sets were less than 10% of the corresponding recorded impact forces. Note that the estimated force shown in Figure 7-a) based on experimentally measured debris velocity which were in the range of 2.37 to 3.24 m/s, while the upper limit of estimated bore velocity (Eqn.2) are 1.40 m/s and 1.66 m/s for the 550 and 850 mm impounding water depths, respectively. Therefore using the estimated debris velocity leads to lower impact forces. Figure 7-b) depicts the estimated debris-impact forces using FEMA P-646 (2012) with four different values for the coefficient c, with the experimentally measured forces for six test sets. For the conditions of a direct longitudinal strike, FEMA P-646 recommends $c = 0$ for wooden log debris. The estimated forces underestimated the recorded forces by 5% to 40% for all tests except for 1kg debris with the 550 mm impounding water depth; the estimated force was 10% higher. For $c = 0.2$ and 0.3 the estimated forces were in close agreement with the recorded forces for the small debris (1kg), but underestimated the forces for other debris. Lastly, good agreement, in general, was achieved with $c = 1.0$. Note, however, that this value of c corresponds to debris oriented transverse to flow direction according to the recommendations of FEMA P-646.

5 CONCLUSIONS

This study is a step towards further understanding of tsunami-bore forces induced on near-shore structures and presents experimental data which will be towards this goal. The force-time histories experienced by the structural models were characterized by three distinct stages of force development: impulsive force caused by leading edge of the bore front impacting the model; run-up force which corresponds to the highest force recorded in each test; and a relatively moderate magnitude hydrodynamic force following the due to the quasi-steady flow state. FEMA P-55 (2011) and P-646 (2012) were used to estimate the hydrodynamic and debris-impact forces and compared against those recorded during testing.

- **Hydrodynamic forces**: The prediction equations for the flow velocity and momentum flux provided in the guidelines were used to calculate the hydrodynamic force. The calculated forces underestimated; however, the forces calculated with FEMA P-55 were closer to the experimentally recorded forces. The forces calculated from FEMA P-646 were less than 15% of the experimental forces. The predicted hydrodynamic forces were significantly improved and both guidelines provided similar results when the experimentally measured bore velocities and bore depths corresponding to the quasi-steady flow state were used.
- **Debris-impact forces**: Although the maximum proposed values for the coefficients of FEMA P-55 were adopted, the calculated impact forces were highly underestimated (less than 10% of the experimental

forces). Four values recommended by FEMA P-646 for the hydrodynamic mass coefficient (0, 0.2, 0.3 and 1.0) were investigated. The largest value was found to provide better estimation of the impact force for large debris (2kg), while the other values for the coefficient were reasonable to estimate the impact forces from small debris (1kg). Note, however, that the mass coefficient of 1.0 is specified for transversely oriented debris, which is not consistent with the longitudinally oriented debris impacts of this study.

REFERENCES

Arikawa, T. 2009. Structural Behavior under Impulsive Tsunami Loading, *Journal of Disaster Research*, vol. 4 No. 6, pp. 377-381.

Asakura R., Iwase K., Ikeya T., Takao M., Fujii N., and Omori M. 2000. An Experimental Study on Wave Force Acting on On-Shore Structures Due to Overflowing Tsunamis, *Proceeding of Coastal Engineering, Japan Society of Civil Engineering,* 47, pp. 911-915.

ASCE, 2010. Minimum Design Loads for Buildings and Other Structures, ASCE/SEI Standard 7-10, *American Society of Civil Engineers*, Reston, Virginia, USA.

Borrero J., Field Survey of Northern Sumatra and Banda Aceh, In-donesia After The Tsunami and Earthquake of 26 December 2004, *Seismological Research Letters*, Vol.76, No.3, pp. 309-318, 2005.

Chock G., Robertson I., Kriebel D., Francis M., and Nistor I., Tohoku Japan Tsunami of March 11, 2011 – Performance of Structures, *Final Report, ASCE* 2012, 297 p.

City and County of Honolulu Building Code (CCH) 2000. Department of Planning and Permitting of Honolulu Hawaii. *Chapter 16 Article 11*. Honolulu, Hawaii.

Federal Emergency Management Agency 2012. Guidelines for Design of Structures for Vertical Evacuation from Tsunamis. *FEMA P-646,* Washington, DC., USA.

Federal Emergency Management Agency 2005, Coastal Construction Manual, *FEMA P-55 Report, Edition 4th*, Washington, D.C. USA.

Fujima, K., Achmad, F., Shigihara, Y., & Mizutani, N. 2009. Estimation of Tsunami Force Acting on Rectangular Structures. *Journal of Disaster Research*, vol. 4 No. 6, pp 4-9.

Fujima K., Shigihara Y., Tomita T., Honda K., Nobuoka H., Hanzawa M., Fujii H., Otani H., Orishimo S., Tatsumi M., and Koshimura S. 2006. Survey results of the Indian Ocean tsunami in the Mal-Dives, *Coastal Engineering Journal*, Vol.48, No.2, pp. 91-97,.

Haehnel, R. B., & Daly, S. F. 2002. Maximum Impact Force of Woody Debris on Floodplain Structures Cold Regions Research and Engineering Laboratory. *Technical Report ERDC/CRREL TR-02-2* US.

Lukkunaprasit, P., Thanasisathit, N., & Yeh, H. 2009. Experimental Verification of FEMA P646 Tsunami Loading, *Journal of Disaster Research* vol. 4 No. 6.

Nouri Y., Nistor I., Palermo D. and Cornett A. 2010, Experimental Investigation of Tsunami Impact on Free Standing Structures. *Coastal Engineering Journal*, JSCE and World scientific, 52 (1); 43-70.

Okada T., Sugano T., Ishikawa T., Ohgi T., Takai S., and Hamabe C., Structural Design Method of Buildings for Tsunami Resistance (SMBTR) 2005, *a code proposed by The Building Technology Research Institute of The Building Center of Japan*.

Oshnack, M. E., & Aguiniga, F., Cox Daniel, Rakesh G., and J. van de L. 2009. Effectiveness of Small Onshore Seawall in Reducing Forces Induced by Tsunami Bore : Large Scale Experimental Study, *Journal of Disaster Research* vol. 4 No. 6, pp 382-390.

Palermo, D., Nistor, I., Al-Faesly, T. and Cornett A. 2012. Impact of Tsunami Forces on Structures: The University of Ottawa Experience, *5th International Tsunami Symposium*, Ispra, Italy.

Saatcioglu M., Ghobarah A., and Nistor I., 2006. Performance of structures in Indonesia during the 2004 Sumatra earthquake and tsunami, *Earthquake Spectra*, 22, pp. 295 - 319.

Yeom, G., Nakamura, T., & Mizutani, N. 2009. Collision Analysis of Container Drifted by Runup Tsunami Using Drift Collision Coupled Model, *Journal of Disaster Research* vol. 4 No. 6, pp 441-449.